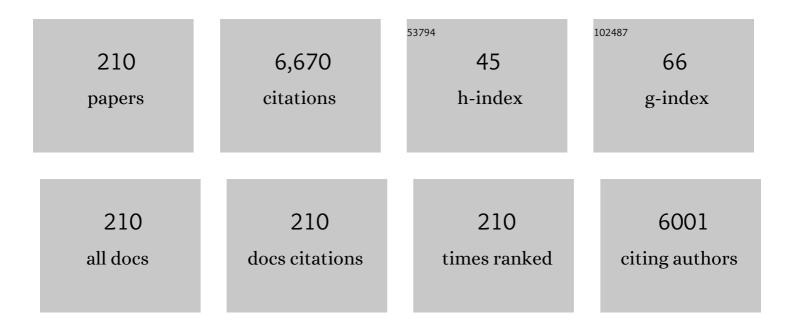
## Xiao-dong Shen

List of Publications by Year in descending order

Source: https://exaly.com/author-pdf/1710899/publications.pdf Version: 2024-02-01



#	Article	IF	CITATIONS
1	Freeze Casting: From Lowâ€Dimensional Building Blocks to Aligned Porous Structures—A Review of Novel Materials, Methods, and Applications. Advanced Materials, 2020, 32, e1907176.	21.0	404
2	Mesoporous amine-modified SiO2 aerogel: a potential CO2 sorbent. Energy and Environmental Science, 2011, 4, 2070.	30.8	214
3	Halideâ€Based Materials and Chemistry for Rechargeable Batteries. Angewandte Chemie - International Edition, 2020, 59, 5902-5949.	13.8	142
4	Highâ€Energy Interlayerâ€Expanded Copper Sulfide Cathode Material in Nonâ€Corrosive Electrolyte for Rechargeable Magnesium Batteries. Advanced Materials, 2020, 32, e1905524.	21.0	125
5	Synthesis of a novel Al2O3–SiO2 composite aerogel with high specific surface area at elevated temperatures using inexpensive inorganic salt of aluminum. Ceramics International, 2016, 42, 874-882.	4.8	115
6	Effects of synthetic C-S-H/PCE nanocomposites on early cement hydration. Construction and Building Materials, 2017, 140, 282-292.	7.2	109
7	Compatibility between a polycarboxylate superplasticizer and the belite-rich sulfoaluminate cement: Setting time and the hydration properties. Construction and Building Materials, 2014, 51, 47-54.	7.2	94
8	Developing Polymer Cathode Material for the Chloride Ion Battery. ACS Applied Materials & Interfaces, 2017, 9, 2535-2540.	8.0	90
9	Nanoconfined Iron Oxychloride Material as a High-Performance Cathode for Rechargeable Chloride Ion Batteries. ACS Energy Letters, 2017, 2, 2341-2348.	17.4	87
10	Relationship between water permeability and pore structure of Portland cement paste blended with fly ash. Construction and Building Materials, 2018, 175, 458-466.	7.2	87
11	Novel Al <sub>2</sub> O <sub>3</sub> –SiO <sub>2</sub> composite aerogels with high specific surface area at elevated temperatures with different alumina/silica molar ratios prepared by a non-alkoxide sol–gel method. RSC Advances, 2016, 6, 5611-5620.	3.6	85
12	A new aerogel based CO <sub>2</sub> adsorbent developed using a simple sol–gel method along with supercritical drying. Chemical Communications, 2014, 50, 12158-12161.	4.1	83
13	Enhanced Ferromagnetism and Tunable Magnetism in Fe <sub>3</sub> GeTe <sub>2</sub> Monolayer by Strain Engineering. ACS Applied Materials & Interfaces, 2020, 12, 26367-26373.	8.0	83
14	Dynamic separation of ultradilute CO2 with a nanoporous amine-based sorbent. Chemical Engineering Journal, 2012, 189-190, 13-23.	12.7	80
15	Research on cement hydration and hardening with different alkanolamines. Construction and Building Materials, 2017, 141, 296-306.	7.2	80
16	Hierarchically ordered mesoporous Co3O4 materials for high performance Li-ion batteries. Scientific Reports, 2016, 6, 19564.	3.3	79
17	Effect of Nano-SiO2 on the Early Hydration of Alite-Sulphoaluminate Cement. Nanomaterials, 2017, 7, 102.	4.1	79
18	Amine hybrid aerogel for high-efficiency CO 2 capture: Effect of amine loading and CO 2 concentration. Chemical Engineering Journal, 2016, 306, 362-368.	12.7	77

#	Article	IF	CITATIONS
19	A novel building material with low thermal conductivity: Rapid synthesis of foam concrete reinforced silica aerogel and energy performance simulation. Energy and Buildings, 2018, 177, 385-393.	6.7	77

A novel all-solid electrolyte based on a co-polymer of poly-(methoxy/hexadecal-poly(ethylene glycol)) Tj ETQq0 0 0 rgBT /Overlock 10 Tf 5

21	Dynamic capture of low-concentration CO2 on amine hybrid silsesquioxane aerogel. Chemical Engineering Journal, 2016, 283, 1059-1068.	12.7	72
22	Development of monolithic adsorbent via polymeric sol–gel process for low-concentration CO2 capture. Applied Energy, 2015, 147, 308-317.	10.1	71
23	Magnesium Anode for Chloride Ion Batteries. ACS Applied Materials & Interfaces, 2014, 6, 10997-11000.	8.0	69
24	Effect of SO3 and MgO on Portland cement clinker: Formation of clinker phases and alite polymorphism. Construction and Building Materials, 2014, 58, 182-192.	7.2	69
25	Hydration Mechanism of Reactive and Passive Dicalcium Silicate Polymorphs from Molecular Simulations. Journal of Physical Chemistry C, 2015, 119, 19869-19875.	3.1	68
26	Polymer-Derived SiOC Integrated with a Graphene Aerogel As a Highly Stable Li-Ion Battery Anode. ACS Applied Materials & Interfaces, 2020, 12, 46045-46056.	8.0	66
27	Preparation of monolith SiC aerogel with high surface area and large pore volume and the structural evolution during the preparation. Ceramics International, 2014, 40, 8265-8271.	4.8	65
28	Influence of core/shell TiO2@SiO2 nanoparticles on cement hydration. Construction and Building Materials, 2017, 156, 114-122.	7.2	64
29	Evolution of the novel C/SiO2/SiC ternary aerogel with high specific surface area and improved oxidation resistance. Chemical Engineering Journal, 2017, 330, 1022-1034.	12.7	63
30	pH-Responsive Magnetic Mesoporous Silica-Based Nanoplatform for Synergistic Photodynamic Therapy/Chemotherapy. ACS Applied Materials & Interfaces, 2018, 10, 15001-15011.	8.0	62
31	Synergistic effect of metakaolin and limestone on the hydration properties of Portland cement. Construction and Building Materials, 2019, 223, 177-184.	7.2	61
32	Relation between reactivity and electronic structure for α′L-, β- and γ-dicalcium silicate: A first-principles study. Cement and Concrete Research, 2014, 57, 28-32.	11.0	59
33	High efficiency photocatalytic conversion of CO <sub>2</sub> with H <sub>2</sub> O over Pt/TiO <sub>2</sub> nanoparticles. RSC Advances, 2014, 4, 44442-44451.	3.6	59
34	Facile preparation of cross-linked polyimide aerogels with carboxylic functionalization for CO 2 capture. Chemical Engineering Journal, 2017, 322, 1-9.	12.7	59
35	Facile synthesis of resorcinol–formaldehyde/silica composite aerogels and their transformation to monolithic carbon/silica and carbon/silicon carbide composite aerogels. Journal of Non-Crystalline Solids, 2012, 358, 3150-3155.	3.1	57
36	Effects of limestone powder on the hydration and microstructure development of calcium sulphoaluminate cement under long-term curing. Construction and Building Materials, 2019, 199, 688-695.	7.2	55

#	Article	IF	CITATIONS
37	Alite-ye'elimite cement: Synthesis and mineralogical analysis. Cement and Concrete Research, 2013, 45, 15-20.	11.0	54
38	Preparation of magnetic MnFe2O4-Cellulose aerogel composite and its kinetics and thermodynamics of Cu(II) adsorption. Cellulose, 2018, 25, 735-751.	4.9	54
39	Effect of fly ash on the pore structure of cement paste under a curing period of 3 years. Construction and Building Materials, 2017, 144, 493-501.	7.2	51
40	A Pyrite Iron Disulfide Cathode with a Copper Current Collector for Highâ€Energy Reversible Magnesiumâ€Ion Storage. Advanced Materials, 2021, 33, e2103881.	21.0	50
41	Synthesis of monolithic mesoporous silicon carbide from resorcinol–formaldehyde/silica composites. Materials Letters, 2013, 99, 108-110.	2.6	49
42	Kinetics of calcium sulfoaluminate formation from tricalcium aluminate, calcium sulfate and calcium oxide. Cement and Concrete Research, 2014, 55, 79-87.	11.0	49
43	Blanket-like Co(OH)2/CoOOH/Co3O4/Cu(OH)2 composites on Cu foam for hybrid supercapacitor. Electrochimica Acta, 2020, 334, 135559.	5.2	49
44	Co-based anode materials for alkaline rechargeable Ni/Co batteries: a review. Journal of Materials Chemistry, 2012, 22, 277-285.	6.7	48
45	Plasma-Induced Synthesis of CuO Nanofibers and ZnO Nanoflowers in Water. Plasma Chemistry and Plasma Processing, 2014, 34, 1129-1139.	2.4	47
46	Facile synthesis of an amine hybrid aerogel with high adsorption efficiency and regenerability for air capture via a solvothermal-assisted sol–gel process and supercritical drying. Green Chemistry, 2015, 17, 3436-3445.	9.0	47
47	Thermal and Mechanical Performances of the Superflexible, Hydrophobic, Silica-Based Aerogel for Thermal Insulation at Ultralow Temperature. ACS Applied Materials & Interfaces, 2021, 13, 21286-21298.	8.0	46
48	Compressive strength and hydration characteristics of high-volume fly ash concrete prepared from fly ash. Journal of Thermal Analysis and Calorimetry, 2019, 136, 565-580.	3.6	45
49	Carbon incorporation effects and reaction mechanism of FeOCl cathode materials for chloride ion batteries. Scientific Reports, 2016, 6, 19448.	3.3	43
50	Preparation and accelerated carbonation of low temperature sintered clinker with low Ca/Si ratio. Journal of Cleaner Production, 2016, 120, 249-259.	9.3	42
51	Flexible and super hydrophobic polymethylsilsesquioxane based silica aerogel for organic solvent adsorption via ambient pressure drying technique. Powder Technology, 2020, 373, 716-726.	4.2	42
52	A new mesoporous amine-TiO2 based pre-combustion CO2 capture technology. Applied Energy, 2015, 147, 214-223.	10.1	41
53	High emissivity MoSi2–ZrO2–borosilicate glass multiphase coating with SiB6 addition for fibrous ZrO2 ceramic. Ceramics International, 2016, 42, 8140-8150.	4.8	41
54	An Allâ€Solidâ€State Rechargeable Chloride Ion Battery. Advanced Science, 2019, 6, 1802130.	11.2	41

#	Article	IF	CITATIONS
55	Interaction effect of triisopropanolamine and glucose on the hydration of Portland cement. Construction and Building Materials, 2014, 65, 360-366.	7.2	40
56	Cation disordered rock salt phase Li2CoTiO4 as a potential cathode material for Li-ion batteries. Journal of Materials Chemistry, 2012, 22, 6200.	6.7	39
57	Ti2Ni alloy: a potential candidate for hydrogen storage in nickel/metal hydride secondary batteries. Energy and Environmental Science, 2010, 3, 1316.	30.8	38
58	Enhancing the addition of fly ash from thermal power plants in activated high belite sulfoaluminate cement. Construction and Building Materials, 2014, 52, 261-266.	7.2	38
59	Amine hybrid zirconia/silica composite aerogel for low-concentration CO2 capture. Microporous and Mesoporous Materials, 2016, 236, 269-276.	4.4	37
60	Properties of Portland cement paste blended with coral sand powder. Construction and Building Materials, 2019, 203, 662-669.	7.2	37
61	Effect of Ti addition on mechanical properties and corrosion resistance of Ni-free Zr-based bulk metallic glasses for potential biomedical applications. Journal of Alloys and Compounds, 2020, 815, 152636.	5.5	37
62	Effect of silica sources on nanostructures of resorcinol–formaldehyde/silica and carbon/silicon carbide composite aerogels. Microporous and Mesoporous Materials, 2014, 197, 77-82.	4.4	36
63	Silica aerogels formed from soluble silicates and methyl trimethoxysilane (MTMS) using CO2 gas as a gelation agent. Ceramics International, 2018, 44, 821-829.	4.8	35
64	Synthesis and textural evolution of mesoporous Si3N4 aerogel with high specific surface area and excellent thermal insulation property via the urea assisted sol-gel technique. Chemical Engineering Journal, 2020, 382, 122880.	12.7	35
65	Influence of CuO on the formation and coexistence of 3CaO·SiO2 and 3CaO·3Al2O3·CaSO4 minerals. Cement and Concrete Research, 2006, 36, 1784-1787.	11.0	34
66	Preparation of SiO <sub>2</sub> aerogel from rice husk ash. RSC Advances, 2015, 5, 65818-65826.	3.6	34
67	Three-dimensional self-supported CuCo <sub>2</sub> O <sub>4</sub> nanowires@NiO nanosheets core/shell arrays as an oxygen electrode catalyst for Li–O <sub>2</sub> batteries. Journal of Materials Chemistry A, 2021, 9, 3007-3017.	10.3	33
68	Direct synthesis of anatase TiO2 aerogel resistant to high temperature under supercritical ethanol. Materials Letters, 2014, 117, 192-194.	2.6	32
69	A new rapid and economical one-step method for preparing SiO2 aerogels using supercritical extraction. Powder Technology, 2017, 312, 1-10.	4.2	32
70	Near-infrared light-activated red-emitting upconverting nanoplatform for T1-weighted magnetic resonance imaging and photodynamic therapy. Acta Biomaterialia, 2018, 74, 360-373.	8.3	32
71	Spherical amine grafted silica aerogels for CO <sub>2</sub> capture. RSC Advances, 2020, 10, 25911-25917.	3.6	32
72	Statistical research on phase formation and modification of alite polymorphs in cement clinker with SO 3 and MgO. Construction and Building Materials, 2012, 37, 548-555.	7.2	31

#	Article	IF	CITATIONS
73	Stability of Tricalcium Silicate and Other Primary Phases in Portland Cement Clinker. Industrial & Engineering Chemistry Research, 2014, 53, 1954-1964.	3.7	31
74	The composition and performance of alite-ye'elimite clinker produced at 1300†°C. Cement and Concrete Research, 2018, 107, 41-48.	11.0	31
75	Research on the formation of M1-type alite doped with MgO and SO3—A route to improve the quality of cement clinker with a high content of MgO. Construction and Building Materials, 2018, 182, 156-166.	7.2	31
76	Modification Effects of Nano-SiO2 on Early Compressive Strength and Hydration Characteristics of High-Volume Fly Ash Concrete. Journal of Materials in Civil Engineering, 2019, 31, .	2.9	31
77	Polyanilineâ€Intercalated FeOCl Cathode Material for Chlorideâ€Ion Batteries. ChemElectroChem, 2019, 6, 1761-1767.	3.4	31
78	Solution plasma synthesis of Pt/ZnO/KB for photo-assisted electro-oxidation of methanol. Journal of Alloys and Compounds, 2017, 692, 848-854.	5.5	30
79	Enhancing Ferromagnetism and Tuning Electronic Properties of Crl <sub>3</sub> Monolayers by Adsorption of Transition-Metal Atoms. ACS Applied Materials & Interfaces, 2021, 13, 21593-21601.	8.0	30
80	Hydration of ternary cement in the presence of triisopropanolamine. Construction and Building Materials, 2016, 111, 513-521.	7.2	29
81	Sulfate adjustment for cement with triisopropanolamine: Mechanism of early strength enhancement. Construction and Building Materials, 2018, 182, 516-522.	7.2	29
82	One-step hydrothermal synthesis of MnOx-CeO2/reduced graphene oxide composite aerogels for low temperature selective catalytic reduction of NOx. Applied Surface Science, 2020, 508, 145024.	6.1	29
83	Chemical Surface Adsorption and Trace Detection of Alcohol Gas in Graphene Oxide-Based Acid-Etched SnO <sub>2</sub> Aerogels. ACS Applied Materials & amp; Interfaces, 2021, 13, 20467-20478.	8.0	29
84	Adsorption properties of nitrobenzene in wastewater with silica aerogels. Science China Technological Sciences, 2010, 53, 2367-2371.	4.0	28
85	Synthesis of a novel porous material comprising carbon/alumina composite aerogels monoliths with high compressive strength. Microporous and Mesoporous Materials, 2013, 172, 182-189.	4.4	27
86	One-step facile synthesis of carbon-supported PdAu nanoparticles and their electrochemical property and stability. Journal of Alloys and Compounds, 2015, 619, 452-457.	5.5	27
87	Electrochemical transformation method for the preparation of novel 3D hybrid porous CoOOH/Co(OH)2 composites with excellent pseudocapacitance performance. Journal of Power Sources, 2019, 443, 227278.	7.8	27
88	A Cu <sub>2</sub> O/Cu/carbon cloth as a binder-free electrode for non-enzymatic glucose sensors with high performance. New Journal of Chemistry, 2020, 44, 1993-2000.	2.8	27
89	Synthesis of a novel three-dimensional Na2SO4@SiO2@Al2O3-SiO2 phase change material doped aerogel composite with high thermal resistance and latent heat. Ceramics International, 2018, 44, 21855-21865.	4.8	26
90	Contribution of core/shell TiO2@SiO2 nanoparticles to the hydration of Portland cement. Construction and Building Materials, 2020, 233, 117127.	7.2	26

#	Article	IF	CITATIONS
91	Effect of surface treatments on microstructure and electrochemical properties of La–Ni–Al hydrogen storage alloy. International Journal of Hydrogen Energy, 2009, 34, 1904-1909.	7.1	25
92	A promising form-stable phase change material composed of C/SiO2 aerogel and palmitic acid with large latent heat as short-term thermal insulation. Energy, 2020, 210, 118478.	8.8	25
93	Microstructure and electrochemical hydrogen storage characteristics of (La0.7Mg0.3)1â^'Ce Ni2.8Co0.5 (x= 0–0.20) electrode alloys. International Journal of Hydrogen Energy, 2011, 36, 3016-3021.	7.1	24
94	Use of one-pot wet gel or precursor preparation and supercritical drying procedure for development of a high-performance CO <sub>2</sub> sorbent. RSC Advances, 2014, 4, 43448-43453.	3.6	24
95	Preparation and Characterization of Polyimide Aerogels with a Uniform Nanoporous Framework. Langmuir, 2018, 34, 10529-10536.	3.5	24
96	The mechanochemical process and properties of Portland cement with the addition of new alkanolamines. Powder Technology, 2015, 286, 750-756.	4.2	23
97	The high capacity and excellent rate capability of Ti-doped Li <sub>2</sub> MnSiO <sub>4</sub> as a cathode material for Li-ion batteries. RSC Advances, 2015, 5, 1612-1618.	3.6	23
98	Influence of borax and citric acid on the hydration of calcium sulfoaluminate cement. Chemical Papers, 2017, 71, 1909-1919.	2.2	23
99	Preparation of amine-modified SiO2 aerogel from rice husk ash for CO2 adsorption. Journal of Porous Materials, 2017, 24, 455-461.	2.6	23
100	Facile preparation of TiO2/ZnO composite aerogel with excellent antibacterial activities. Materials Letters, 2019, 234, 253-256.	2.6	23
101	Hydrophobic in-situ SiO2-TiO2 composite aerogel for heavy oil thermal recovery: Synthesis and high temperature performance. Applied Thermal Engineering, 2021, 190, 116745.	6.0	23
102	Statistical study of cement additives with and without chloride on performance modification of Portland cement. Progress in Natural Science: Materials International, 2011, 21, 246-253.	4.4	22
103	Use of monolithic silicon carbide aerogel as a reusable support for development of regenerable CO <sub>2</sub> adsorbent. RSC Advances, 2014, 4, 64193-64199.	3.6	22
104	Synthesis and characterization of LiMnPO4/C nano-composites from manganese(ii) phosphate trihydrate precipitated from a micro-channel reactor approach. RSC Advances, 2014, 4, 25625.	3.6	22
105	Nanostructured cation disordered Li <sub>2</sub> FeTiO <sub>4</sub> /graphene composite as high capacity cathode for lithium-ion batteries. Materials Technology, 2016, 31, 537-543.	3.0	22
106	Co-polyimide aerogel using aromatic monomers and aliphatic monomers as mixing diamines. Journal of Sol-Gel Science and Technology, 2018, 88, 386-394.	2.4	22
107	Realization of an Ultrahigh Power Factor and Enhanced Thermoelectric Performance in TiS <sub>2</sub> via Microstructural Texture Engineering. ACS Applied Materials & Interfaces, 2020, 12, 41687-41695.	8.0	22
108	A Highâ€Energy Aqueous Manganese–Metal Hydride Hybrid Battery. Advanced Materials, 2020, 32, e2001106.	21.0	22

#	Article	IF	CITATIONS
109	Low-Temperature Liquid Phase Synthesis of Flower-like NiCo <sub>2</sub> O <sub>4</sub> for High-Efficiency Methanol Electro-oxidation. ACS Applied Energy Materials, 2020, 3, 9076-9082.	5.1	22
110	Hydration properties of the alite–ye'elimite cement clinker synthesized by reformation. Construction and Building Materials, 2015, 99, 254-259.	7.2	21
111	Preparation and thermal shock resistance of high emissivity molybdenum disilicide- aluminoborosilicate glass hybrid coating on fiber reinforced aerogel composite. Applied Surface Science, 2017, 416, 805-814.	6.1	21
112	Water Adsorption on the $\hat{I}^2$ -Dicalcium Silicate Surface from DFT Simulations. Minerals (Basel,) Tj ETQq0 0 0 rgBT /	Overlock 2.0	10 Tf 50 622
113	Monolithic silicon nitride-based aerogels with large specific surface area and low thermal conductivity. Ceramics International, 2019, 45, 16331-16337.	4.8	21
114	Amine grafted cellulose aerogel for CO2 capture. Journal of Porous Materials, 2021, 28, 93-97.	2.6	21

115	Modeling, analysis of interaction effects of several chemical additives on the strength development of silicate cement. Construction and Building Materials, 2010, 24, 1937-1943.	7.2	20
116	Use of a Robust and Inexpensive Nanoporous TiO <sub>2</sub> for Pre-combustion CO <sub>2</sub> Separation. Energy & Fuels, 2013, 27, 6938-6947.	5.1	20
117	Solution plasma method for the preparation of Cu-Ni/CuO-NiO with excellent methanol electrocatalytic oxidation performance. Applied Surface Science, 2020, 513, 145808.	6.1	20
118	Facile and Eco-Friendly Synthesis of Finger-Like Co3O4 Nanorods for Electrochemical Energy Storage. Nanomaterials, 2015, 5, 2335-2347.	4.1	19
119	Hydration of Portland cement with alkanolamines by thermal analysis. Journal of Thermal Analysis and Calorimetry, 2018, 131, 37-47.	3.6	19
100	Preparation and characterization of C/Al2 O3 composite aerogel with high compressive strength and		

120	low thermal conductivity. Journal of Porous Materials, 2015, 22, 1235-1243.	2.6	18
121	Investigation on textural and structural evolution of the novel crack-free equimolar Al2O3-SiO2-TiO2 ternary aerogel during thermal treatment. Ceramics International, 2017, 43, 4188-4196.	4.8	18
122	Synthesis and characterization of monolithic carbon/silicon carbide composite aerogels. Journal of Porous Materials, 2013, 20, 845-849.	2.6	17
123	Facile synthesis of TiO2/Ag composite aerogel with excellent antibacterial properties. Journal of Sol-Gel Science and Technology, 2018, 86, 590-598.	2.4	17
124	Cation substitution induced reactivity variation on the tricalcium silicate polymorphs determined from first-principles calculations. Construction and Building Materials, 2019, 216, 239-248.	7.2	17
125	Hybrid Sn–Co binary oxide nanosheets grown on carbon paper as the supercapacitor electrode materials. Journal of Alloys and Compounds, 2020, 814, 152199.	5.5	17
126	Surface organic modification of Fe3O4 magnetic nanoparticles. Journal Wuhan University of Technology, Materials Science Edition, 2008, 23, 436-439.	1.0	16

#	Article	IF	CITATIONS
127	Facile preparation of ZrCO composite aerogel with high specific surface area and low thermal conductivity. Journal of Sol-Gel Science and Technology, 2018, 86, 383-390.	2.4	16
128	Study on the physical and chemical properties of Portland cement with THEED. Construction and Building Materials, 2019, 213, 617-626.	7.2	16
129	Morphology prediction of portlandite: Atomistic simulations and experimental research. Applied Surface Science, 2020, 502, 144296.	6.1	16
130	Electrochemical energy storage of Co powders in alkaline electrolyte. Electrochimica Acta, 2010, 55, 1169-1174.	5.2	15
131	Improved microwave dielectric properties of Mg4Nb2O9 ceramics with CaO–B2O3–SiO2 glass additions. Journal of Materials Science: Materials in Electronics, 2013, 24, 3546-3550.	2.2	15
132	An economic and scalable approach to synthesize high power LiFePO4/C nanocomposites from nano-FePO4 precipitated from an impinging jet reactor. Journal of Materials Chemistry A, 2013, 1, 10429.	10.3	15
133	Low-Temperature Synthesis of LiFePO <sub>4</sub> Nanoplates/C Composite for Lithium Ion Batteries. Energy & Fuels, 2020, 34, 11597-11605.	5.1	15
134	High mass loading Ni4Co1-OH@CuO core-shell nanowire arrays obtained by electrochemical reconstruction for alkaline energy storage. Nano Research, 2022, 15, 685-693.	10.4	15
135	Isocyanate-crosslinked silica aerogel monolith with low thermal conductivity and much enhanced mechanical properties: Fabrication and analysis of forming mechanisms. Ceramics International, 2021, 47, 26668-26677.	4.8	15
136	Electrochemical hydrogen storage properties of a non-equilibrium Ti2Ni alloy. RSC Advances, 2012, 2, 2149.	3.6	14
137	Preparation and adsorption property of phenyltriethoxysilane modified SiO2 aerogel. Journal Wuhan University of Technology, Materials Science Edition, 2013, 28, 916-920.	1.0	14
138	Paclitaxel modified Fe <sub>3</sub> O <sub>4</sub> loaded albumin nanoparticles as drug delivery vehicles by self-assembly. RSC Advances, 2016, 6, 43284-43292.	3.6	14
139	Effect of welan gum on the hydration and hardening of Portland cement. Journal of Thermal Analysis and Calorimetry, 2018, 131, 1277-1286.	3.6	14
140	Halogenidâ€basierte Materialien und Chemie für wiederaufladbare Batterien. Angewandte Chemie, 2020, 132, 5954-6004.	2.0	14
141	Properties of eco-friendly coral sand powder – Calcium sulfoaluminate cement binary system. Construction and Building Materials, 2020, 263, 120181.	7.2	14
142	Effect of Mechanical Milling on the Structure and Electrochemical Properties of Ti2Ni Alloy in an Alkaline Battery. Energy & Fuels, 2009, 23, 4678-4682.	5.1	13
143	Characterization and stability of a new, high-capacity amine-functionalized CO2 sorbent. International Journal of Greenhouse Gas Control, 2013, 18, 51-56.	4.6	13
144	Effect of isothermal annealing on mechanical performance and corrosion resistance of Ni-free Zr59Ti6Cu17.5Fe10Al7.5 bulk metallic glass. Journal of Non-Crystalline Solids, 2020, 537, 120013.	3.1	13

#	Article	IF	CITATIONS
145	NO2 detection and redox capacitance reaction of Ag doped SnO2/rGO aerogel at room temperature. Journal of Alloys and Compounds, 2021, 886, 161287.	5.5	13
146	Robust monolithic polymer(resorcinol-formaldehyde) reinforced alumina aerogel composites with mutually interpenetrating networks. RSC Advances, 2019, 9, 22942-22949.	3.6	12
147	Synthesis of bulk BaTiO3 aerogel and characterization of photocatalytic properties. Journal of Sol-Gel Science and Technology, 2019, 90, 313-322.	2.4	12
148	Reaction of Portland cement clinker with gaseous SO2 to form alite-ye'elimite clinker. Cement and Concrete Research, 2019, 116, 299-308.	11.0	11
149	Polyvinylidene fluoride aerogel with high thermal stability and low thermal conductivity. Materials Letters, 2020, 259, 126890.	2.6	11
150	Effect of coral powder and ground-granulated blast‑furnace slag on the hydration behavior of cement paste. Journal of Thermal Analysis and Calorimetry, 2022, 147, 6643-6654.	3.6	11
151	Adsorption capacity of hydrophobic SiO2 aerogel/activated carbon composite materials for TNT. Science China Technological Sciences, 2013, 56, 1767-1772.	4.0	10
152	One-pot sol–gel synthesis of amine hybrid titania/silsesquioxane composite aerogel for CO2 capture. Journal of Sol-Gel Science and Technology, 2017, 84, 422-431.	2.4	10
153	Enhancing strength and plasticity of Zr-based bulk metallic glasses by Zr partially substituted Fe and isothermal annealing. Journal of Non-Crystalline Solids, 2020, 543, 120163.	3.1	10
154	Alite-ye'elimite clinker: Hydration kinetics, products and microstructure. Construction and Building Materials, 2021, 266, 121062.	7.2	10
155	The low temperature fabrication of nanocrystalline MgAl2O4 spinel aerogel by a non-alkoxide sol-gel route. Materials Letters, 2017, 207, 137-140.	2.6	9
156	Resol and urea derived N-doped porous carbon for Na-ion storage. Materials Chemistry and Physics, 2020, 254, 123535.	4.0	9
157	Distinct anisotropy and a high power factor in highly textured TiS <sub>2</sub> ceramics <i>via</i> mechanical exfoliation. Chemical Communications, 2020, 56, 5961-5964.	4.1	9
158	Multiscale investigation of olivine (0 1 0) face dissolution from a surface control perspective. Applied Surface Science, 2021, 549, 149317.	6.1	9
159	Composition design for high C3S cement clinker and its mineral formation. Journal Wuhan University of Technology, Materials Science Edition, 2007, 22, 56-60.	1.0	8
160	Influences of low-Ti substitution for La and Mg on the electrochemical and kinetic characteristics of AB3-type hydrogen storage alloy electrodes. Science China Technological Sciences, 2010, 53, 242-247.	4.0	8
161	Electrochemical redox mechanism of Co–B–H anode material and its optimization by a novel electrolyte additive. RSC Advances, 2013, 3, 1327-1331.	3.6	8
162	Mechanically reinforced composite aerogel blocks by self-growing nanofibers. RSC Advances, 2014, 4, 48601-48605.	3.6	8

#	Article	IF	CITATIONS
163	Spinel LiMn2â^'x Si x O4 (x < 1) through Si4+ substitution as a potential cathode material for lithium-ion batteries. Science China Materials, 2016, 59, 558-566.	6.3	8
164	Long-term hydration behavior and pore structure development of cement–limestone binary system. Journal of Thermal Analysis and Calorimetry, 2021, 143, 843-852.	3.6	8
165	Effect of gypsum dosage on the hydration and strength of alite-ye'elimite cement synthesized at 1300°C. Construction and Building Materials, 2021, 287, 123063.	7.2	8
166	Shape-tailorable amine grafted silica aerogel microsphere for CO2 capture. Green Chemical Engineering, 2020, 1, 140-146.	6.3	8
167	Preparation and adsorption property of hydrophobic SiO2 aerogels modified by methyl triethoxysilane. Journal Wuhan University of Technology, Materials Science Edition, 2011, 26, 1079-1083.	1.0	7
168	Preparation of fiber reinforced porous silicon carbide monoliths. Materials Letters, 2013, 110, 141-143.	2.6	7
169	Influence of low-dose chemicals on the early strength of Portland cement: statistical and calorimetric evidence. Advances in Cement Research, 2017, 29, 155-165.	1.6	7
170	Triconstituent co-assembly to hierarchically porous carbons as high-performance anodes for sodium-ion batteries. Journal of Alloys and Compounds, 2019, 771, 140-146.	5.5	7
171	Synthesis of hydrophobic silica aerogel and its composite using functional precursor. Journal of Porous Materials, 2020, 27, 295-301.	2.6	7
172	Study of Hydration and Microstructure of Mortar Containing Coral Sand Powder Blended with SCMs. Materials, 2020, 13, 4248.	2.9	7
173	Synthesis of Fe-doped NiO nanosheets on carbon cloth for improved catalytic performance in Li–O <sub>2</sub> batteries. New Journal of Chemistry, 2022, 46, 1601-1607.	2.8	7
174	Synthesis of SnO2nanoparticles using a solution plasma and their gas-sensing properties. Japanese Journal of Applied Physics, 2016, 55, 01AE17.	1.5	6
175	Controllable Low-Temperature Hydrothermal Synthesis and Gas-Sensing Investigation of Crystalline SnO2 Nanoparticles. Journal of Materials Engineering and Performance, 2016, 25, 1342-1346.	2.5	6
176	Kinetics of calcium sulfoaluminate with 1% iron oxide by isothermal and isoconversional methods. Advances in Cement Research, 2017, 29, 336-346.	1.6	6
177	Effects of Nano-CSH on the hydration process and mechanical property of cementitious materials. Journal of Sustainable Cement-Based Materials, 2022, 11, 378-388.	3.1	6
178	Synthesis and characterization of amino-grafted attapulgite/graphene oxide nanocomposites and their adsorption for Pb(II) removal. Journal of Nanoparticle Research, 2022, 24, 1.	1.9	6
179	Effect of barium oxide on the formation and coexistence of tricalcium silicate and calcium sulphoaluminate. Journal Wuhan University of Technology, Materials Science Edition, 2009, 24, 457-461.	1.0	5
180	Analysis of variance for testing method of cement in determination of strength. Progress in Natural Science: Materials International, 2011, 21, 341-346.	4.4	5

#	Article	IF	CITATIONS
181	Effect of germanium on electrochemical performance of chain-like Co–P anode material for Ni/Co rechargeable batteries. Transactions of Nonferrous Metals Society of China, 2013, 23, 2060-2065.	4.2	5
182	Facile synthesis of monolithic carbon/alumina composite aerogels with high compressive strength using different inorganic aluminium salts. Journal of Porous Materials, 2014, 21, 653-658.	2.6	5
183	Welan gum retards the hydration of calcium sulfoaluminate. Journal of Thermal Analysis and Calorimetry, 2017, 130, 899-908.	3.6	5
184	Incorporation of ultrafine nanograins in Zr–Cu–Al–Ni–Co bulk metallic glass enabling significantly improved mechanical properties. Materials Research Express, 2019, 6, 085211.	1.6	5
185	Preparation of ZrC@Al2O3@Carbon composite aerogel with excellent high temperature thermal insulation performance. SN Applied Sciences, 2019, 1, 1.	2.9	5
186	Effect of protogenetic alkali sulfates on the hydration and hardening of cement with different tricalcium aluminate content. Construction and Building Materials, 2020, 256, 119475.	7.2	5
187	Research on structure modulation of alite and its effect on the mechanical properties of cement clinker. Construction and Building Materials, 2021, 303, 124511.	7.2	5
188	A facile process for preparation of polyaniline/polyacrylic acid composite electrochromism films. High Performance Polymers, 2011, 23, 489-493.	1.8	4
189	Preparation of PAA/WO <sub>3</sub> composite films with enhanced electrochromism via layer-by-layer method. Science and Engineering of Composite Materials, 2018, 25, 565-569.	1.4	4
190	Preparation and Organic Solvent Adsorption of PTFE Fabric Reinforced GO/SiO <sub>2</sub> Aerogel. Chemistry Letters, 2020, 49, 1324-1328.	1.3	4
191	Carbon Nanotube Supported Li-Excess Cation-Disordered Li1.24Fe0.38Ti0.38O2 Cathode with Enhanced Lithium-Ion Storage Performance. Journal of Electronic Materials, 2021, 50, 5029-5036.	2.2	4
192	Effect of CuO on the formation mechanism of calcium sulphoaluminate. Journal Wuhan University of Technology, Materials Science Edition, 2008, 23, 518-521.	1.0	3
193	Formulation design of the multi-component cement additive by using engineering statistics. Journal Wuhan University of Technology, Materials Science Edition, 2010, 25, 538-544.	1.0	3
194	Electrochemical properties of Co-S/x wt.% AB5 composite materials. Science China Technological Sciences, 2015, 58, 1355-1359.	4.0	3
195	The effect of gaseous SO2 secondary sintering on the cement composition and crystal structure. Construction and Building Materials, 2021, 285, 122872.	7.2	3
196	Preparation and properties of crystallizable Glass/Al2O3 composites for LTCC material. Journal Wuhan University of Technology, Materials Science Edition, 2011, 26, 1174-1178.	1.0	2
197	Synergistic interactions of chemical additives on the strength development of silicate cement by a boxâ€behnken model optimization. Journal of Applied Polymer Science, 2014, 131, .	2.6	2
198	Diffusion characteristic of sulfate anion in surface region of cement mortar at early stage. Journal Wuhan University of Technology, Materials Science Edition, 2017, 32, 358-364.	1.0	2

#	Article	IF	CITATIONS
199	Strengthening Effect of Short Carbon Fiber Content and Length on Mechanical Properties of Extrusion-Based Printed Alumina Ceramics. Materials, 2022, 15, 3080.	2.9	2
200	Preparation of paclitaxel-loaded microspheres with magnetic nanoparticles. Frontiers of Materials Science in China, 2007, 1, 383-387.	0.5	1
201	Notice of Retraction: Application of Central Composite Design to process optimization of Fe <sub>3</sub> O <sub>4</sub> /SiO <sub>2</sub> composited aerogel nanoparticle. , 2010, , .		1
202	Optimization of the content of tricalcium silicate of high cementing clinker. Journal Wuhan University of Technology, Materials Science Edition, 2011, 26, 578-582.	1.0	1
203	Polymorph transformation kinetics of Ca3SiO5with MgO. Phase Transitions, 2015, 88, 888-896.	1.3	1
204	Supercritical drying: a promising technique on synthesis of sorbent for CO <sub align="right">2 capture. International Journal of Clobal Warming, 2017, 12, 228.</sub>	0.5	1
205	Effects of limestone powder on the early hydration of tricalcium aluminate. Journal of Thermal Analysis and Calorimetry, 0, , 1.	3.6	1
206	Partially Reduced TiO <sub>2</sub> Aerogel as a Catalyst of Oxygen Reduction Reaction in Alkaline Solution. Chemistry Letters, 2022, 51, 862-866.	1.3	1
207	Modeling and estimation of the kinetics of seeded solvent-mediated phase transformation in a batch crystallizer. Journal Wuhan University of Technology, Materials Science Edition, 2011, 26, 872-878.	1.0	0
208	Development of a new calcium sulfoaluminate (synthetic ye'elimite) blended PII 52.5 cement. Advances in Cement Research, 2017, 29, 373-386.	1.6	0
209	Molecular reorientation in a dehydration process of an organic polar salt of 2,4-diaminotoluene/L(+)-tartaric acid. Powder Diffraction, 2017, 32, 15-22.	0.2	0
210	Remarkable enhancement in the electrochemical properties of cosmetic brush-like Co <sub>3</sub> O <sub>4</sub> nanowires via <i>in situ</i> surface modification with Ni <sup>2+</sup> . Nanotechnology, 2020, 31, 365405.	2.6	0